JOINT TIME FREQUENCY ANALYSIS TECHNIQUES: A STUDY OF TRANSITIONAL DYNAMICS IN SHEET/CLOUD CAVITATION

Morten Kjeldsen
Norwegian University of Science
and Technology
N7491 Trondheim, Norway
Morten.Kjeldsen@maskin.ntnu.no

Roger E. A. Arndt
St. Anthony Falls Laboratory
University of Minnesota
Mississippi River at 3rd AVE SE
Minneapolis, MN 55414
arndt001@tc.umn.edu

Abstract

An introduction to, and the use of, Joint Time Frequency Analysis techniques is given. Special emphasis is made on Time Frequency Distribution series. This method is demonstrated on selected experimental data. Attention is given the transition region in the dynamic nature of sheet/cloud cavitation. Wavelets and a method that is a variation of phase-portraits are also presented and discussed with regard to cavitation dynamics. An example on how experimental techniques have been improved by the above mentioned methods is given.

1 Introduction

A comprehensive mapping of cavitation dynamics on a NACA 0015 Hydrofoil has been undertaken by Kjeldsen *et al* (2000), Arndt *et al* (2000a) and (2000b), and Arndt and Levy (2000). This work has been motivated by the fact that high performance hydraulic systems can operate at partial cavitating conditions leading to increased levels of dynamical structural loading in addition to the potential danger of cavitation erosion. This paper is considered complementary to other publications by the authors cited above.

In order to cope with many of the phenomena encountered in the study a number of signal analysis tools were employed. Of special interest was the ability to observe signal evolution in both time and frequency. Joint Time Frequency Analysis (JTFA) techniques were introduced. This enabled other methods for mapping the dynamic characteristics. Additionally this technique lead to other experimental techniques and discussions on the system dynamics. It must be emphasized that JTFA tools have been utilized before in the naval/cavitation community. Ng (1991) used Wigner-Ville distributions in the analysis of temporal dynamics of cavitating pumps and valves, and Fahrat (1994) used wavelet analysis for the investigation of pressure dynamics on a cavitating hydrofoil.

This paper will also utilize methods of displaying dynamics known from the mathematical field of dynamical systems. This type of analysis is given as an indication that the dynamics of sheet/cloud cavitation is indeed going through a transition.

It's important to stress that the methods presented are on an applied level, while the fundamentals of the mentioned methods are given scant attention.

2 Problem statement

Early in the study of dynamics on a NACA 0015 hydrofoil (c=81mm) a change in dynamics at a value of the composite cavitation index $\sigma/2\alpha \approx 4$ was identified. This change manifested itself in the spectral content as

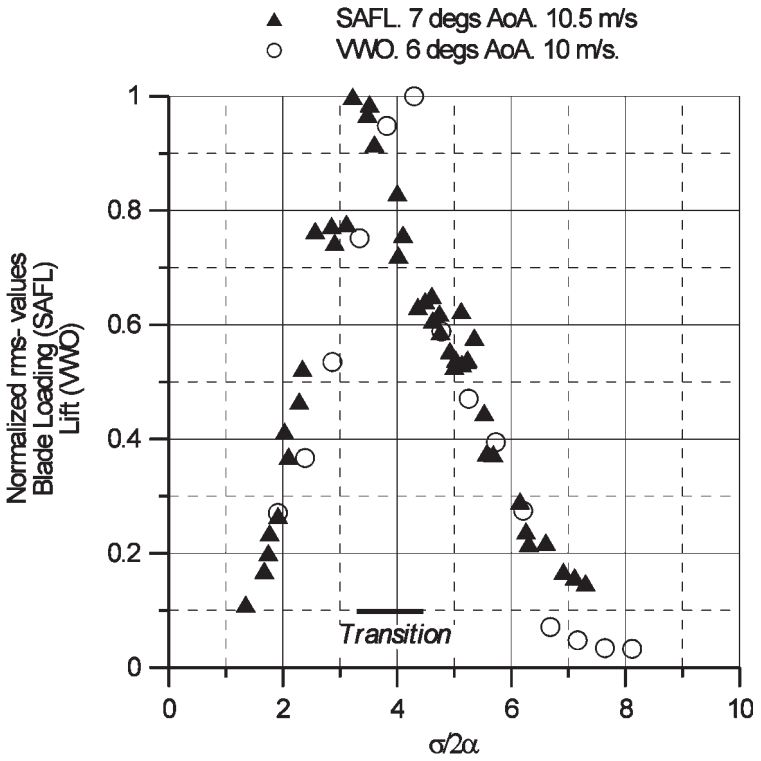

Figure 1: Level of cavitation induced unsteadiness as a function of the composite parameter $\sigma/2\alpha$. The transition is defined for the interval of the composite parameter where the level of oscillation is peaking.

well in the level of lift oscillations, Figure 1. This change occurs at $l/c \approx 3/4$ and corresponds to that found theoretically by Watanabe *et al* (1998).

Furthermore the investigators distinguished between two dynamic regimes, see e.g. Arndt *et al* (2000a).

- Type I: For $\sigma/2\alpha < 4$, the dynamics is governed by shock wave physics. The dominant frequency can be found as: $fc/U \approx 0.25$, c being the chord length.
- Type II: For $\sigma/2\alpha > 4$, the dynamics is governed by re-entrant jet physics. The dominant frequency can be found as: $fl/U \approx 0.3$, l being the cavity length.

A third domain for higher values of $\sigma/2\alpha$ has also been identified, consisting of low frequency oscillations at sheet inception.

During the study, questions were raised whether some of the spectral characteristics of Type I dynamics could be attributed to the dynamic response of the water tunnel. Therefore similar studies were made at two different tunnels; the water tunnel at the St. Anthony Falls Laboratory (SAFL), and a scaled up version (c=129mm) of the same experiment at the Versuchsanstalt für Wasserbau- Obernach (VWO). As shown in Figure 1 a good correspondence between measurements at the two locations was found. Different approaches on measurements were applied for the two set-ups:

- Lift: Early measurements at SAFL and all measurements at VWO included fluctuating lift.
- Blade loading: Measured as the difference between two pressure transducers mounted on the pressure and suction side on the base of the hydrofoil. This constituted the bulk of measurements at SAFL. These types of measurements were validated by comparing spectra with those of simultaneous accelerometer readings. The accelerometer was mounted inside the hydrofoil.
- Surface pressure: An array of pressure transducers mounted on one side of the foil was used for measurement of the dynamics. These measurements have been the focus of recent SAFL investigations.

3 Joint Time Frequency Analysis

3.1 Prerequisites

Regular Fourier transforms provide an efficient tool to observe a signal in frequency space. The obvious fallacy with a Fourier transform is the fact that the algorithm is an average of the frequency content over time. In effect the use of regular Fourier transforms is at best when analysis of steady oscillatory signals are made. If a piece of music was to be transformed into the frequency domain a knowledge of the location in time for each frequency is needed. The music community acknowledges this fact and displays the frequency (note) as a function of time (beat) on their musical sheets.

The engineering community has also overcome the short-comings of FFT. One method is the "water-fall" where the original (discrete) temporal signal is divided into (overlapping) sub-domains upon which the Fourier transform is made. This is in practice the same method as using a windowed Fourier transform, or short time Fourier transform (STFT):

$$STFT\,(t,\omega) = \int_t s(\tau)\gamma(t-\tau)e^{-i\omega\tau}d\tau \tag{1}$$

Where γ defines the window function. Although Equation 1 indicates a continuous integral, the result and the actual algorithm will be discrete. Furthermore the resolution in both time and frequency will have to obey an uncertainty principle.

According to Qian and Chen (1996), Gabor stated that if a signal was to be represented simultaneously in the time and frequency domains the following general expansion is valid:

$$f(t) = \sum_m \sum_n C_{m,n} h_{m,n}(t) \tag{2}$$

This expansion, known as the Gabor expansion is also the starting point for most JTFA techniques. It can further be shown that, when $h(t)$, e.g. $h(t) = \gamma(t-\tau)e^{-i\omega\tau}$, is complete the coefficients $C_{m,n}$ will be those of the STFT, Equation 1.

In order to make a spectrogram, analogous to the power spectrum of Fourier analysis, the Wigner-Ville transform (WVD) is used on the r.h.s. of Equation 2. Further we define a zone of influence (order) in the discrete frequency/ time lattice using Manhattan distance as the metric. This will be a deviation from direct WVD transforms, and the result will be time frequency distribution series (TFDS) that can be considered as a compromise between STFT and pure WVD. The terms to be calculated are, Qian and Chen (1996):

$$\begin{aligned}
TFDS_D\,(t,\omega) &= \sum_{d=0}^{D} P_d(t,\omega) \\
P_d(t,\omega) &= \sum_{|m-m'|+|n-n'|=d} C_{m,n}C_{m',n'}WVD_{h,h'}(t,\omega), h_{m,n}(t) = \left(\frac{\alpha}{\pi}\right)^{\frac{1}{4}} e^{-\frac{\alpha}{2}(t-mT)^2+jn\Omega t} \\
WVD_{h,h'}(t,\omega) &= 2e^{-\alpha\left(t-\frac{m+m'}{2}T\right)^2-\frac{1}{\alpha}\left(\omega-\frac{n+n'}{2}\Omega\right)^2} e^{-i\frac{n+n'}{2}\Omega(m-m')} e^{i\left[(m-m')T\omega+(n-n')\Omega t\right]}
\end{aligned}$$

Now Ω and T define the discretisation in frequency and time respectively. It should be mentioned that the direct Wigner-Ville, defined as the integral over all cross-correlations, has an infinite zone of influence ($D \to \infty$). For the JTFAs used in this paper the order three ($D = 3$) has been used consequently. The software LabView from National Instruments was used to perform the calculations.

3.2 Ramping techniques

Since one of the tasks was to investigate the dynamic characteristics of a hydrofoil, the active use of ramping of the system pressure was tested. These experiments were made using the pressure loading measurement technique at SAFL. In practice the ramp was made by either slightly opening the vacuum or pressure line connected the vessel controlling the system pressure. Analogous measurements were made by ramping the

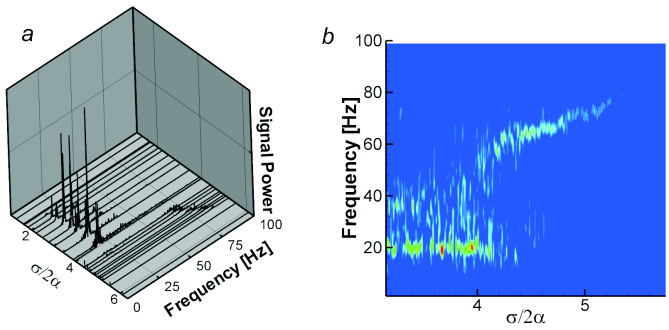

Figure 2: The spectral content is similar even if found by traditional means (a) or by ramping the system pressure (b). Ramping duration $\approx 30s$, $\alpha = 7^0$ and $U = 10m/s$ for both (a) and (b). At transition, $\sigma/2\alpha \approx 4$, a change from type I to type II dynamics is found. Colors (b) indicate amplitudes.

pump speed. In Figure 2 the ramping is being compared with traditionally obtained spectra, the latter being made while running the SAFL tunnel at stable conditions, for various cavitation numbers.

The ramping technique, together with the traditional mapping, concluded in two important findings:

- The frequency domain signal "fingerprint" changed over the transition region as defined in Figure 1. The two dynamic regions defined previously are found.
- The technique of ramping the cavitation index captures quite well qualitative aspects of the dynamics as compared with traditionally obtained spectra.

During the ramping experiments, hystheresis was also searched for in the transition from one to the other dynamic region. These investigations were made by approaching the transition region from above or below. For the current measurements and analysis the resolution and accuracy are too coarse to state whether hysteresis in the transition region exist.

3.3 Studies of dynamics at transition

The region of transition has been submitted to investigation using the JTFA techniques oultlined above. Again the spectral content is of primary importance.

When transition occurs at $\sigma/2\alpha \approx 4$ the cavity length normalized by the chord length is: $l/c = 3/4$. The expression for the main spectral component for Type II dynamics (re-entrant jet physics), $fl/U \approx 0.3$, can be rewritten ,when substituting c for l, as: $fc/U \approx 0.4$. This is close to the first superharmonic of Type I dynamics (shock-wave physics), where the main spectral component is given as: $fc/U \approx 0.25$.

A jump to the first superharmonic is more evident in the VWO data-sets, while at SAFL jumps to the second superharmonic of Type I dynamics were found, Figure 2.

One of the important findings is that the frequencies corresponding to the two mentioned dynamic regimes are preferrably appearing separate in time, see Figures 3, 4 and Figure 7. The authors have yet to conclude whether these regimes can co-exist, and if so, whether a lock-in of the phenomena can occur amplifying the unsteadiness of the cavitating flow. Indeed the use of JTFA techniques is promising for further investigation into the problems of transitional dynamics.

4 Mapping of dynamics

A typical time trace from any measurement will contain a number, N, of local maxima and minima, $p(n)$. If we define the mapping:

$$p_{n+1} = f(p_n), n \in (0, N-1) \tag{3}$$

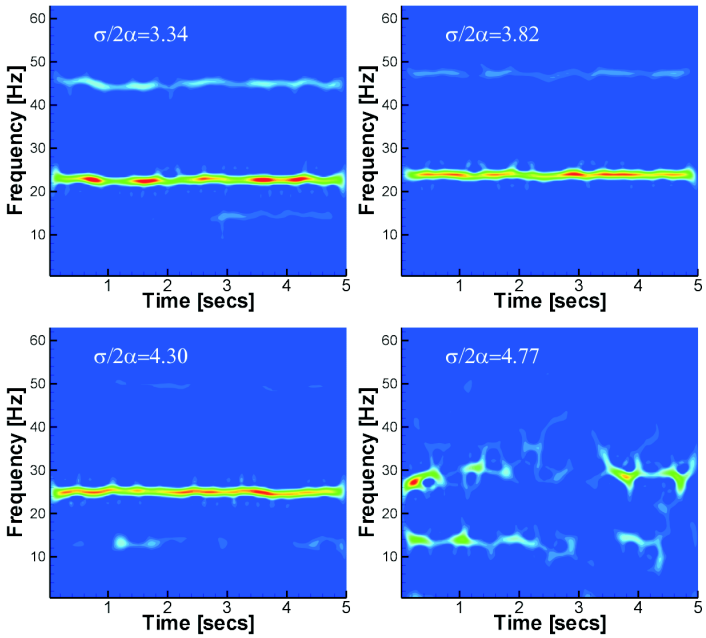

Figure 3: JTFA analysis of lift measurements at VWO, $f_s = 1kHz$ and $n_s = 5000$, unfiltered. For all measurements $\alpha = 6^0, U_0 = 10m/s$ and $c_g = 17.1\%$. Amplitudes are normalized.

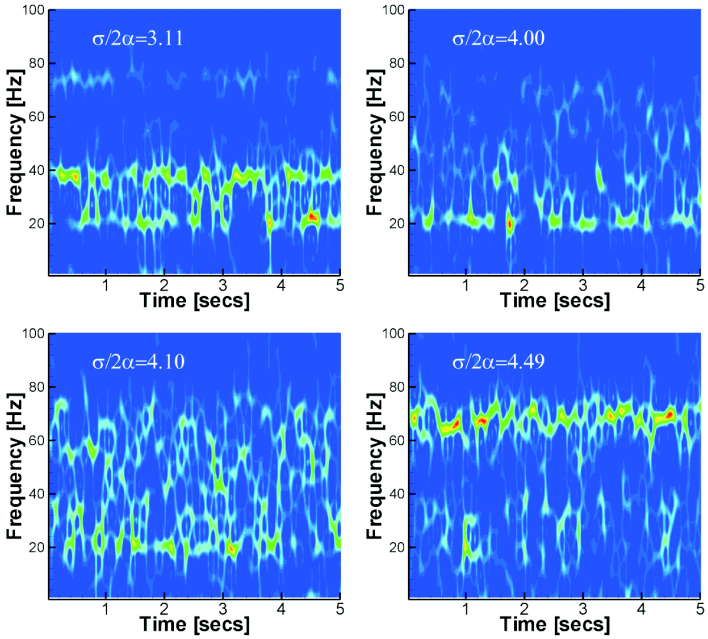

Figure 4: JTFA analysis of blade loading measurements at SAFL, $f_s = 5kHz$ and $n_s = 32768$, unfiltered. For all measurements $\alpha = 7^0$ and $U = 10m/s$. Amplitudes are normalized.

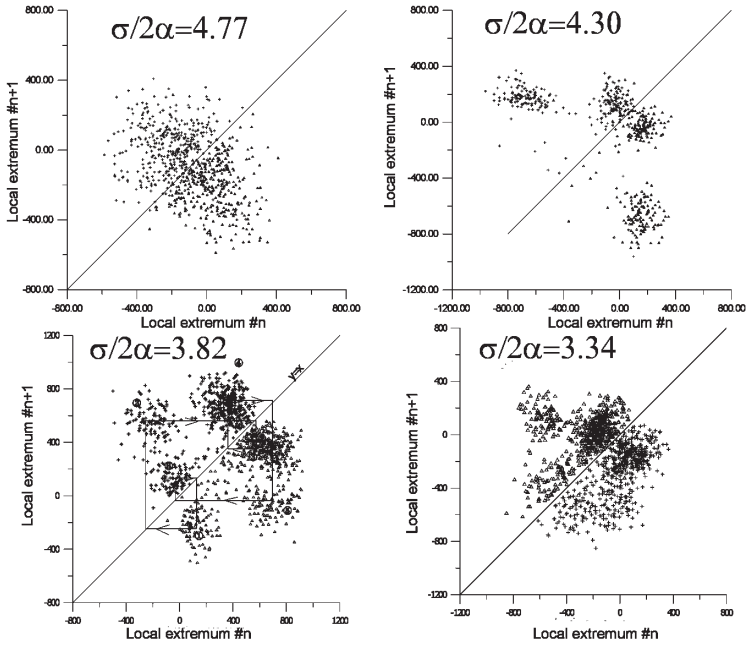

Figure 5: One interpretation is that bifurcations occurs in the data-sets (more points of return develop), thus indicating a transition to a chaotic state. For all measurements $\alpha = 6^0, U_0 = 10m/s$ and $c_g = 17.1\%$. Corresponds to measurements in Figure 3

A phase plot can be made that reveals some of the dynamics. If for a continuous differential equation a finite number of fixed points appear, the phase plot will reveal the existence of a cyclic solution, i.e. $p_{n+1} = p_{n-j}$ for a given j. If an infinite number of return points (p_{n+1}'s) appear, i.e. $p_{n+1} \neq p_{n-j}$ for any j, a chaotic solution exists. These facts have been demonstrated by one the current authors (MK) by solving the Duffing Equation for different parameter settings. Furthermore it has been demonstrated that the transition to chaos is associated with rapid bifurcations, see e.g. Young (1980) p.138.

The outlined philosophy has been applied to some of the lift measurements made at VWO. In Figure 5 the results of the above mentioned analysis are displayed. The authors have to underscore the fact that this type of analysis will to some extent be obscured by the fact that these are analyses of experimental signals. For the current analysis the best conclusion is that regions in the "p_n" space define return points. For the practical analysis a sub-routine within the LabView environment was used to extract the local extremum. This specific algorithm will detect local extremum if the signal conform to certain constraints within an analysis window. On the other hand a manual intervention has to be made in the post-processing in order to avoid "peak-peak" sequences in the data set.

When comparing Figure 5 with Figure 3 it must be remarked that period 2 oscillations for e.g. data set at $\sigma/2\alpha = 4.30$ can actually be represented by two different period 1 oscillations for finite periods of time.

5 Wavelet analysis

Wavelets have been introduced in several scientific fields over the past decades. As with Fourier techniques and JTFA, wavelet analysis is based on orthogonal decomposition of the original signal. Use of wavelets and wavelet analysis include analysis of temporal data as well as analysis of multi-dimensional data, e.g. a number of wavelet-based picture compression routines have been developed.

For our purpose of investigating temporal data, the difference will be in the base function used for the orthogonal decomposition. A "mother" or analysis wavelet,$\psi(t)$, that satisfy specific constraints, will define the complete set of wavelets that are needed to make a time-frequency representation of the temporal signal. A wavelet is finite in time, unlike the trigonometric functions, making wavelets more favorable for the analysis

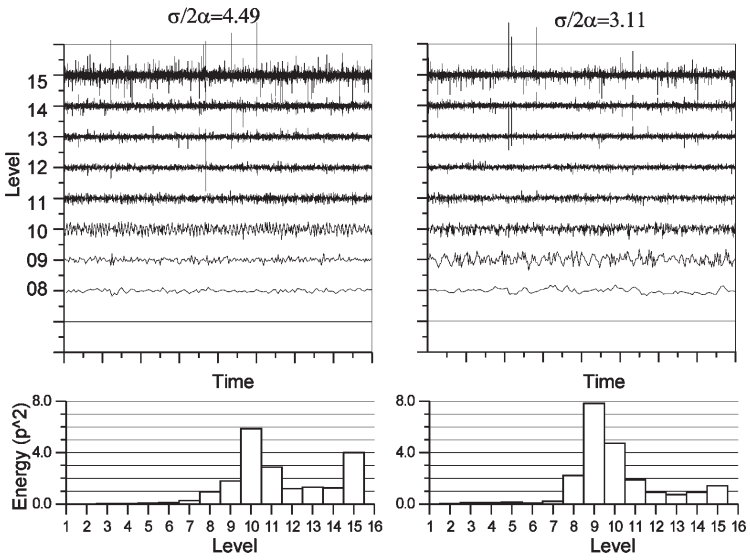

Figure 6: Wavelet analysis of SAFL data. The original signals have been split into a number of levels after Wavelet filter action and downsampling. Higher levels contain higher frequencies, and more samples. $f_s = 5kHz$, $n_s = 32768$, $U = 10m/s$ and $\alpha = 6^0$

of transient signals. A wavelet analysis will in practice allow studies of the original signal localized in both time (due to the shift) and frequency (due to scaling). The definition of the continuous wavelet's shift and scaling can be expressed as, Strang and Nguyen (1998):

$$\psi_{jk}(t) = 2^{\frac{-j}{2}} \psi\left(2^j t - k\right) \tag{4}$$

In the cited equation the $j-$index determines the scaling while the $k-$index defines the shift. The set of wavelets will define a base from which an orthogonal decomposition of the original signal can be made in analogy to the Fourier analysis:

$$\begin{aligned} f(t) &= \sum_{j,k} b_{jk} \psi_{jk}(t) \\ b_{jk} &= \int_{-\infty}^{\infty} f(t) \psi_{jk}(t)\, dt \end{aligned} \tag{5}$$

The coefficients b_{jk} will now represent the signal strength in both time (k-index) and frequency (j-index). This type of analysis will be similar to the JTFA techniques presented previously, except for the fact that the frequency/ time lattice will be unevenly distributed compared with the one used together with JTFA.

For the discrete analysis the wavelet can be attributed a filter (matrix), where the dilatations will be calculated after downsampling the once filtered remaining signal. This leads to the attractive feature that the original signal can be investigated at different scales or frequencies. The sequences of low pass and high pass filtering will be determined by the wavelet filter coefficients (high pass) and complementary scaling functions (low pass).

This utility of wavelet analysis has been used on two data-sets consisting of the instantaneous blade loading on the SAFL hydrofoil. In Figure 6 details, given by the action of the wavelet filter, are shown.

A natural question is whether there is any gain from utilizing wavelets from more traditional bandpass filter techinques. One of the authors of Kumar and Foufoula (1997) explained this by stating that: 1. Wavelet analysis also provides location information.2 It can't be guaranteed that the band pass filters will capture "independent" information. Orthogonal wavelet transforms capture independent information. That is why when a full decomposition of the signal is done, the number of wavelet coefficients are the same as the original signal length and they can be recombined to reconstruct the original signal.

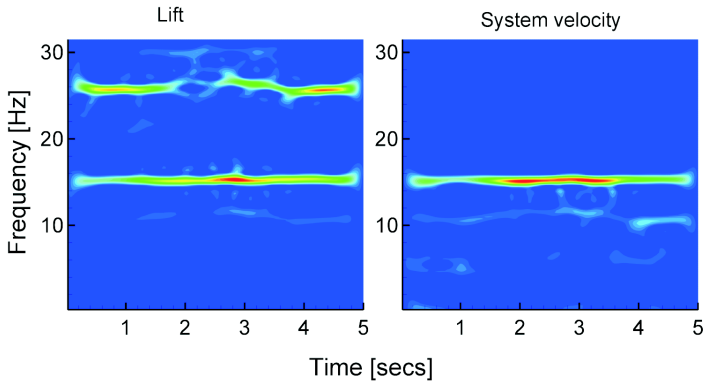

Figure 7: The system velocity based on measured pressure difference shows a strong spectral component within the same period of time that the lift produces the same frequency. Measurements of lift made at VWO, $\sigma/2\alpha = 3.34, \alpha = 6^0, U_0 = 11.9m/s$ and $c_g = 17.1\%$.

Regarding the latter statement the following is also valid for the energy displayed in Figure 6:

$$\sigma_f^2 = \sum_J \sigma_j^2 \tag{6}$$

Where σ_j is the energy at level j. The energy content at each level will also be decisive for where dynamics is occuring. These facts allows a study of the signal evolution at each level. Figure 6, shows the evolution of the signal at independent levels as a function of time. As expected, the energy content is found at lower frequencies/levels when the cavitation number is below transition.

6 Tunnel system dynamics

Since type I dynamics apparantly had a constant shedding frequency for cavitation numbers lower than transition, a study was made to find out whether tunnel system dynamics could be an unwanted influence on the measurements. Early indications had shown that the shedding frequencies could show up in the pressure measurements made for determination of the cavitation index, see Figure 7.

Based on these supiscions a larger measurement program was completed at SAFL, where the dynamic pressure at various positions along the loop were sampled simultaneously as the dynamic surface pressure. These measurement were repeated for a number of cavitation numbers, and at various pump speeds or test section velocities. A preliminary analysis shows that the shedding frequency is present in the tunnel loop. Further analysis and conclusions of the program will be presented in Kjeldsen *et al* (2001).

7 Conclusions

This paper has outlined in greater detail the analysis techniques used for the study of partial cavitation at SAFL and VWO. An important observation is that partial cavitation can't be treated as a steady oscillatory phenomenon even in controlled closed circuits. This observation has lead to an extensive use of Joint Time-Frequency domain analysis. JTFA's based on a compromise between Wigner-Ville distributions and Short Time Fourier transforms have been outlined in greater detail. The resulting analysis tool, Time Frequency Distribution Series, has been applied succesfully to different aspects of partial cavitation.

A cost-effective method of mapping dynamics over a range of cavitation numbers using ramping in system pressure and post processing with JTFA have been demonstrated. Although a similar method can be applied to cavitation testing of pumps and turbines no such efforts have been made yet by the authors.

The use of return maps from dynamical systems has also been demonstrated. Although some inherent problems using these together with experimental data exist, further studies will be made to see if these plots can reveal some of the dynamics in the intermediate states at transition. At present, indications are that the

partial cavitation system undergoes a transition that has similiarities to the "bifurcation route to chaos". To continue on this path will require extremely controlled laboratory conditions, and/or refinements of the experimental set-up and the signal processing tools.

A brief introduction to wavelets has been given, and applications on some of the data collected has been demonstrated. Although the aspect of multiresolution was the scope here, it's believed that wavelet analysis can play a significant role in cavitation research and for diagnostic tools.

The use of the presented analysis tools in this paper is considered crucial for obtaining insight into the phenomena at transitional dynamics in sheet/cloud cavitation. It must be emphasized that visual studies constitutes a major part of the analysis program, but has not been outlined in this text.

Acknowledgements

This work was supported by the National Science Foundation.

References

Arndt R.E.A. Keller A. and Kjeldsen M. 2000a Unsteady Operation Due to Cavitation *Proceedings. Hydraulic Machinery and Systems 20th IAHR Symposium*, Charlotte, NC, August

Arndt R.E.A. Song C.C.S. Kjeldsen M. He J. and Keller A. 2000b Instability of Partial Cavitation: A Numerical/Experimental Approach *Proceedings Twenty-Third Symposium on Naval Hydrodynamics*, Val de Reuil, France, Sept.

Arndt R.E.A. and Levy M. 2000 Acoustic Radiation From Cavitating Hydrofoils *Proceedings, Seventh International Congress on Noise and Vibration*, Garmisch, Germany, July

Fahrat M. 1994 Contribution a l'étude de l'érosion de cavitation: Mecanismes hydrodynamiques et prédiction. *Thesis no 1273, École Polytechnique Fédérale de Lausanne.*

Kjeldsen M. Arndt R.E.A. and Effertz M. 2000 Spectral Characteristics of Sheet/ Cloud Cavitation *Journal of Fluids Engineering*, **122**, No. 3, Sept.

Kjeldsen M. Arndt R.E.A. and Svingen B. 2001 Transients in closed loop hydraulic systems *To be presented IAHR WG-meeting*, Trondheim, Norway, June.

Kumar P. and Foufoula-Georgiou E. 1997 Wavelet analysis for geophysical applications *Reviews of Geophysics,* **35**, 4/ November 1997, pp. 385-412.

Ng K. W. 1991 Diagnostic of Cavitation in Pumps and Valves Using the Wigner Distribution. *FED Cavitation and Multiphase Flow Forum, ASME* **109**

Qian S. and Chen D. 1996 Joint time-frequency analysis: Methods and applications *Prentice Hall*

Strang G. and Nguyen T. 1998 Wavelets and Filter banks *Wellesley- Cambridge Press.*

Watanabe S. Tsujimoto Y. Franc J.P. and Michel J.M. 1998 Linear Analysis of Cavitation Instabilities *Proceedings of Third International Symposium on Cavitation* Grenoble, France, April.

Young F. R. 1989 Cavitation. *McGraw-Hill*